
NEW TECHNOLOGIES OF PREPARATION
AND TREATMENT OF MATERIALS

Preparation of Silicon Nitride and Oxonitride by Gas-Phase Pyrolysis of Hexamethyldisilazane

N. A. Ovsyannikov^{a, *}, Yu. F. Kargin^{a, **}, A. S. Lysenkov^{a, ***}, N. A. Alad'ev^a,
S. N. Ivicheva^{a, ****}, and K. A. Solntsev^{a, *****}

^a*Baikov Institute of Metallurgy and Materials Science, Russian Academy of Sciences, Moscow, 119334 Russia*

**e-mail: nikovs@mail.ru*

***e-mail: yukargin@imet.ac.ru*

****e-mail: toxa55@bk.ru*

*****e-mail: ivicheva@mail.ru,*

******e-mail: solntsev@pran.ru*

Received May 13, 2019; revised May 28, 2019; accepted May 30, 2019

Abstract—The technique was developed, the installation was done, and the conditions for the production of Si_3N_4 and $\text{Si}_2\text{N}_2\text{O}$ by the method of gas-phase pyrolysis of hexamethyldisilazane $(\text{CH}_3)_3\text{-Si-NH-Si-(CH}_3)_3$ (HMDS) were experimentally studied. In the experiments, two different methods of inputting the raw material were used—the input of a vapor–gas mixture (bubbling feeder with heating to supply the HMDS vapor in a stream of carrier gases) and input as a gas-droplet stream (pneumatic nozzle). The effect of gas-dynamic synthesis conditions at temperatures up to 1100°C on the properties of silicon oxonitride and silicon nitride nanopowders was studied. The influence of the conditions of mixing the reactants, the volume ratio of nitrogen/ammonia, and the content of HMDS in the vapor–gas mixture on the yield of products was shown. The dependences of the degree of conversion of the feedstock on the gas flow rate and the concentration of ammonia in the gas phase were obtained. The optimal conditions for the pyrolysis process were found: temperature, the ratio of the components of the gas mixture, the conditions of mixing, and the contact times of the phases. X-ray amorphous Si_3N_4 and $\text{Si}_2\text{N}_2\text{O}$ powders with particle sizes of 50–200 nm and a specific surface area of up to $15\text{ m}^2/\text{g}$ and powders of alpha modification of silicon nitride Si_3N_4 in the form of threadlike crystals with a particle diameter of 50–200 nm were obtained.

Keywords: silicon nitride, silicon oxonitride, pyrolysis, hexamethyldisilazane

DOI: 10.1134/S2075113320020288

INTRODUCTION

In the silicon–nitrogen system, there is only one chemical compound—silicon nitride of the composition Si_3N_4 . The current state of development of materials based on silicon nitride is described in detail in [1–18]. Si_3N_4 is a refractory compound with a predominantly covalent type of interatomic bond. The melting point of silicon nitride is about 1900°C , at which decomposition takes place into Si and N_2 . At 1800°C , dissociation starts, and at 1900°C , silicon nitride completely dissociates into silicon and nitrogen in a wide pressure range [2, 19–21]. Three crystalline polymorphic modifications of Si_3N_4 are known: α -, β -, and γ - Si_3N_4 . The alpha- and beta-silicon nitride crystallize in trigonal (space group $P31c$) and hexagonal (space group $P6_3/m$) syngonies and have the same phenacite structural type [22–25]. The gamma-silicon nitride crystallizes in cubic syngony [26–28] and is of the spinel structural type (space group $Fd3m$). The main structural element of α - and

β - Si_3N_4 is SiN_4 tetrahedra bonded by common nitrogen atoms and located at a relative angle of 120° . The chain arrangement of tetrahedra makes silicon nitride isomorphic to many silicate minerals, which determines the possibility of formation of complex phases in the Si–Al–O–N system (for example, sialons).

There are several methods for the synthesis of silicon nitride: furnace—direct nitriding of silicon at 1000 – 1500°C ; nitriding in plasma flow; reduction of SiO in the presence of nitrogen; reaction of SiH_4 with nitrogen in the presence of ammonia; gas phase deposition in $\text{SiCl}_4 + \text{NH}_3 + \text{C}_3\text{H}_8 + \text{H}_2$, $\text{SiH}_4 + \text{NH}_3 + \text{CH}_4 + \text{H}_2$ systems, etc.; thermal degradation of silazanes $\text{R}_n\text{Si-NH-SiR}_m$, alkylaminoboranes R_3NBH , methacarborene $\text{C}_2\text{B}_{10}\text{H}_{12}$, decaborane $\text{B}_{10}\text{H}_{14}$ in the presence of ammonia, hydrogen, and nitrogen. In particular, there are reports on the use of hexamethyldisilazane (HMDS) for the preparation of silicon oxycarbonitride films of variable composition $\text{SiC}_x\text{N}_y\text{O}_z\text{:H}$ by plasma-chemical decomposition [29], amorphous

Si/C/N powders by laser spray pyrolysis [30], and SiBN ceramics by pyrolysis of polyborosilazane [31].

The purpose of this work is the synthesis of silicon nitride and oxonitride powders using hexamethyldisilazane (HMDS, $C_6H_{19}NSi_2$, structural formula $(CH_3)_3-Si-NH-Si-(CH_3)_3$, boiling point of $125^\circ C$, density of 0.75 g/cm^3) by gas phase pyrolysis.

EXPERIMENTAL

Experiments on the preparation of silicon nitride and oxonitride were carried out by the method of pyrolysis of organometallic compounds (OMC) in a quartz reactor. The installation includes the following main units: quartz pyrolytic reactor 1 m in length and 70 mm in diameter; a system for drying, dosing, and feeding nitrogen and ammonia into the reactor; a non-contact type feedstock evaporator; a feed unit for feeding the reactor; and a quenching and capture system for the finished product—fine powders of silicon nitride and oxonitride on a bag filter. To compensate the increasing pressure in the system caused by an increase in gas-dynamic resistance of the bag filter as it operates, a vacuum pump is provided at the outlet. Two different methods of introducing raw materials were used in the experiments—introduction of a vapor–gas mixture (a bubbler feeder with heating to supply HMDS vapor in a carrier gas stream) and introduction in the form of a gas-droplet stream (pneumatic nozzle). This is due to the fact that, upon obtaining composite materials, the initial reactants often have very different boiling points, which makes impossible their combined supply to the reactor in the vapor–gas form. Introduction in the form of a gas-droplet stream allows one to use combined mixtures of organic and inorganic substances that have different physical properties (boiling point, vapor pressure, solubility, etc).

The installation works as follows. A temperature close to the boiling point of HMDS ($125^\circ C$) was set in the bubbler feeder, and the flow was fed into the reactor through the central channel of the input device. The amount of raw material fed to the reactor was controlled by temperature in the evaporator and the flow rate and temperature of the carrier gas. At the same time, a nitrogen–ammonia mixture preheated to $125^\circ C$ was fed coaxially into the reactor through a ring channel of a larger diameter. The volumetric ratio of nitrogen/ammonia was varied from 1/3 to 1/10 with a total flow rate of 2 to 8 L/min. Owing to the tangentially located inlet of the mixture of nitrogen and ammonia, a rotational movement is imparted. Such a device made it possible to stabilize the feed stream, preventing it from dispersing prematurely in the zone of relatively low temperatures at the inlet of the reactor; to shield the near-wall regions of the reactor from excessive subsidence of the skull layer of the target product near the feed inlet; and also to improve mix-

ing conditions of the reagents in the zone of working temperatures by increasing the flow turbulence. The resulting vapor–gas mixture was sent to a pyrolytic reactor, in which the temperature of $800\text{--}1100^\circ C$ was maintained. Silicon nitride (or oxonitride) resulting from pyrolysis was collected on a filter.

In the case of the gas–droplet method, the feedstock was preliminarily prepared for introduction into the pyrolytic reactor. For this, the corresponding amounts of hexamethyldisilazane (HMDS) and tetraethoxysilane (TEOS) were mixed. Separately, with vigorous stirring at the rate of not more than 20 mL/min, a 5% solution of anhydrous lanthanum formate in butanol-1 was introduced into aluminum sec-butoxide (ASB). Immediately before synthesis, the prepared solutions were mixed. The lanthanum formate was introduced from the calculation of the final oxide content in silicon oxonitride at the level of 0.2–1.0 wt %. Before use, REE formate was dried in vacuum at a temperature of not more than $180\text{--}200^\circ C$ until complete removal of traces of moisture. The temperature in the reactor ranged from 600 to $1150^\circ C$. Solid pyrolysis products were captured using a bag filter made of quartz fabric. To feed raw materials into the reactor, a specially developed three-channel pneumatic nozzle was used. Raw materials were introduced through a tube of the central channel of the nozzle with a diameter of 1 mm under excess pressure of 1–1.5 atm. Through a coaxially located annular channel under pressure of 3–3.5 atm, a nebulizer gas (carrier) was supplied—nitrogen, the flow of which undergoes rotational motion as described previously. The channel gap is about 0.5 mm. The shape of the spray torch, i.e., its width and length, was controlled by the position of the cutoff of the central channel relative to the annular channel and the flow rate of the gas spray, so that it would minimize the reflux of raw materials onto the walls of the reactor near the input point, since this effect is very critical in the implementation of the process. According to the results of experiments on a model solution, the viscosity and density of which is similar to the actual working composition, the optimal values of the carrier gas flow rate and the cutoff values of the central feed channel are found, which provide a spray cone width of no more than the inner diameter of the reactor, which allows minimizing the casting of raw materials to the walls of the reactor.

Regardless of the composition of the initial mixture, the behavior of individual droplets during their passage along the axis of the reactor can be represented as several successive stages. The first stage is rapid heating of the droplet; the second stage is evaporation of volatile components of the initial mixture, i.e., organometallic compounds (HMDS, TEOS) and organic solvent. At the same time, as temperature rises, thermal decomposition of nonvolatile components of the mixture (REE formate) proceeds and they mix with gaseous nitrogen and ammonia. The third stage is the actual pyrolysis of components, which fol-

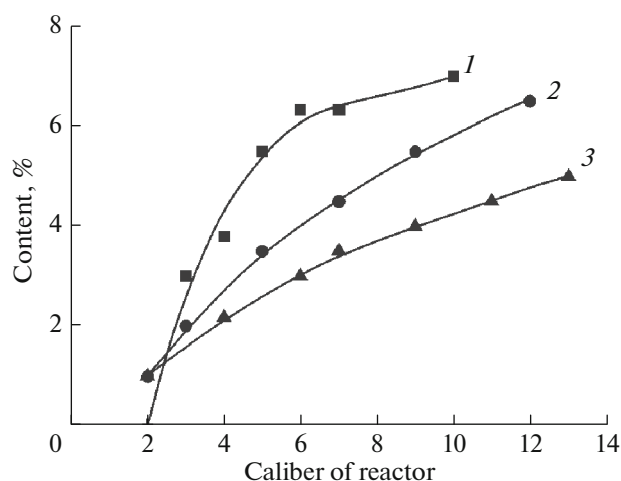


Fig. 1. The change in the content of pyrolysis products in the gas phase along the length reactor depending on the flow rate of the carrier gas, L/min: (1) 2, (2) 3, (3) 4.

lows the general mechanism—evolution of gaseous products—methane, ethane, saturated and unsaturated hydrocarbons of the C₂–C₄ series, and hydrogen; and the formation of a solid phase—nitride, oxide, oxonitride, partially silicon carbide, REE oxide, and carbon black.

The heating of the droplet stream and its evaporation cause a noticeable drop in temperature in the reactor. With a decrease in the droplet size and, correspondingly, with an increase in their total surface, the heating efficiency and evaporation rate increase. The best conditions for spraying raw materials are achieved with a carrier gas flow rate of 2–3 L/min. The second and third stages are accompanied by a significant increase in the volume of the gas phase because of the release of gaseous pyrolysis products. In this case, the average gas flow rate increases, and the residence time of the components of the mixture in the reaction zone decreases, which can lead to a slippage of raw material and reduction of the degree of its conversion. A change in the volume of the components of the gas mixture (ammonia and nitrogen) also affects this parameter. To study the influence of these effects on the pyrolysis process, measurements of the temperature and composition of the gas phase in the axial section of the reactor were carried out, and the degree of conversion of the feedstock was studied depending on the gas-dynamic mixing conditions of the reactants, the contact time of the reacting components, and the state of aggregation of the products of pyrolysis. It is experimentally established that, in the synthesis mode, there is a decrease in temperature (to 400°C) at a distance of 2.5 calibers of the reactor (about 200 mm) from the nozzle cut. The effect is associated with a sharp absorption of heat during the evaporation of droplets of raw material (first stage). Next, the temperature profile enters the operating mode. The analysis of the

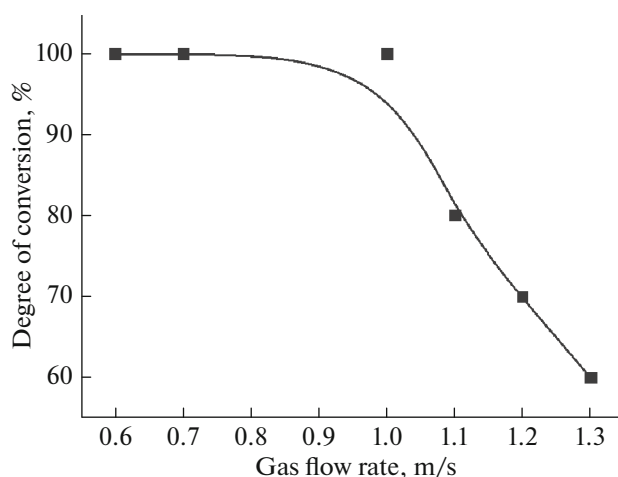


Fig. 2. Dependence of the degree of conversion of the feedstock on the gas flow rate.

composition of the gas phase was carried out using a water-cooled quartz tube probe, which was introduced from the end of the reactor and moved in the axial direction. Scanning at the sampling points was carried out with a step of 70 mm (d of the reactor). Analysis of samples was performed with an ALTAIR 5X gas analyzer. At a distance of 250 mm from the nozzle cut in the gas samples, traces of pyrolysis products—carbon monoxide, methane, ethane and ethylene, hydrogen—were detected, and then their concentration uniformly increased along the length of the reactor and became maximal. The content of gaseous pyrolysis products in the gas samples along the axis of the reactor for different values of the carrier gas flow rate at the pyrolysis temperature of 1100°C is shown in Fig. 1.

At the flow rate of the carrier gas about 2 L/min, the spraying conditions reduce the number of droplets with a size of more than 0.06–0.08 mm to 25%; the reaction under these conditions ends at 8–10 calibers of the reactor. At the flow rate of the carrier gas of 4 L/min and more, despite high-quality atomization (the content of droplets with a size of more than 0.08 mm was less than 5%), because of the high flow rate, the pyrolysis reaction within the reactor length does not end; there is a slippage of unreacted raw material. The dependence of the degree of conversion of raw material on the gas flow rate is shown in Fig. 2.

Under the best conditions of dispersion (consumption of the carrier gas is 2–2.5 L/min), one should consider the optimal flow rate to be no more than 0.8–1 m/s, while conversion is about 100%.

The pyrolysis of OMC (apparently, both oxygen-containing and oxygen-free) results from the elimination of the radicals RO and R from the initial molecules. Considering this mechanism of thermal decomposition, one can propose a scheme of radical interaction reactions that describe the formation of all

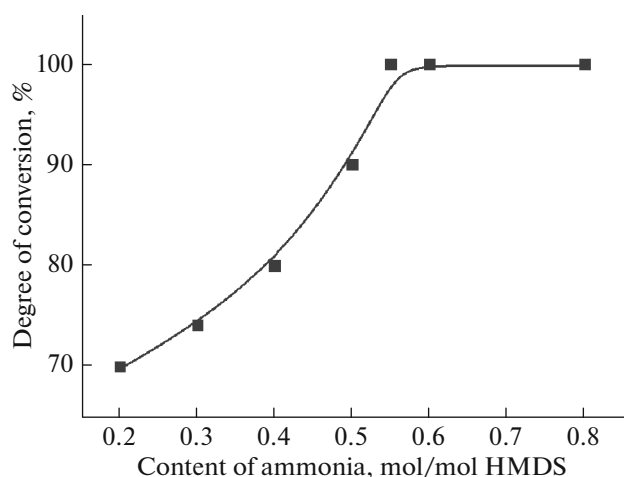


Fig. 3. Dependence of the degree of conversion on the concentration of ammonia in the gas phase.

experimentally detected pyrolysis products. At temperatures of 600–700°C, reactions of the interaction of radicals with the formation of alcohols, saturated and unsaturated hydrocarbons, and water dominate. At temperatures above 1000°C, the primary process of decomposition of primary radicals (R and RO) occurs with the formation of the simplest compounds—carbon monoxide, methane, ethane, and elemental carbon. Under the same temperature conditions, ammonia also undergoes partial decomposition with the formation of NH and NH₂ radicals. Ammonia is a component of the mixture, which, on one hand, promotes a shift in the equilibrium of the pyrolysis reaction toward the formation of nitrides and, on the other hand, acts as an inhibitor of the formation of soot carbon. The latter effect is explained by the formation of alkyl amines R_n-NH_{3-n}, which helps to reduce the concentration of the carbon-forming component of the gas phase—ethylene.

As a result, when ammonia is introduced into the system, an increase in the degree of conversion of raw material is observed. Complete conversion is achieved when the ammonia content is not less than 0.5–0.6 mol per 1 mol of the feedstock. Figure 3 shows the general dependence of the degree of conversion of raw material, calculated on the basis of the gas phase composition, depending on the ammonia content in the gas phase.

To identify the phase and chemical composition of the samples of the obtained powders, the methods of X-ray diffraction (XRD, XRD 6000 Shimadzu diffractometer, CuK_α radiation, graphite monochromator, λ = 1.540598 Å) and IR spectroscopy (Nicolet iS5 IR spectrometer) were used. The microstructure and morphological features of the samples were studied using scanning electron microscopy (SEM) (LEO 1420 electron microscope, JEOL).

RESULTS AND DISCUSSION

The determining parameter of the gas-phase pyrolysis process is the degree of conversion, which depends on the process temperature, gas-dynamic mixing conditions of the reactants, contact time of the reacting components, and the aggregation state of the pyrolysis products. The study of the pyrolysis patterns was carried out in the range of operating temperatures of 950–1050°C. It is found that, at the average gas flow rate in the reactor of less than 1 m/s (the residence time of the reactants in the reactor is about 1 s), the degree of conversion is 100%. At high rates, this indicator decreases rapidly, since the vapor–gas mixture with decrease in the residence time in the reaction zone does not have time to warm up sufficiently—a breakthrough of the unreacted raw material to the filter occurs. At the optimal gas flow rate (less than 1 m/s), the fullness of the conversion is achieved only at the ammonia content of at least 0.5–0.6 mol per 1 mol of HMDS. Increasing the volume of ammonia above this value does not cause any changes. At the same time, the worsening of the conditions for mixing of gaseous reactants caused by the decrease in the total volume of the nitrogen–ammonia mixture leads to a decrease in the degree of conversion even under conditions of a sufficient amount of the supplied ammonia. With an increase in the flow rate of the nitrogen–ammonia mixture, a slip is observed. The best mixing conditions are achieved when the volume of the nitrogen–ammonia mixture exceeds the volume of the vapor–gas mixture (feed + carrier gas) by 8–12 times.

Thus, the optimal conditions of the synthesis of silicon nitride for the dimensions of the pyrolytic reactor used in the experiments at a temperature of 1000°C are determined: the consumption of HMDS is not more than 200 mL/h, the carrier gas consumption flow rate is about 3 L/min, and the flow rate of the nitrogen–ammonia mixture should exceed the volume of the vapor–gas mixture (raw material + carrier gas) by 8–12 times at the ammonia content of at least 0.5–0.6 mol per 1 mol of HMDS feed to the reactor.

Experiments on the use of the gas-droplet method of injection by means of a nozzle showed similar results. However, the optimal residence time of the reagents providing 100% conversion should be at least 1.5–1.7 s. This, apparently, is due to significant heat losses associated with the need for heating and evaporation of the feedstock.

The dispersed Si₂N₂O powder obtained by the pyrolysis of HMDS according to the XRD data is X-ray amorphous with the specific surface area of about 15 m²/g and bulk density of 0.2–0.25 g/cm³. According to the SEM images (Fig. 4), the synthesized powder has spherical particles with an average size of 10–40 nm and, according to the particle size analysis (Fig. 5), is prone to agglomeration. The pore size calculated by the Barrett–Joyner–Halenda (BJH) method is 2 nm (i.e., micropores predominate). According to the

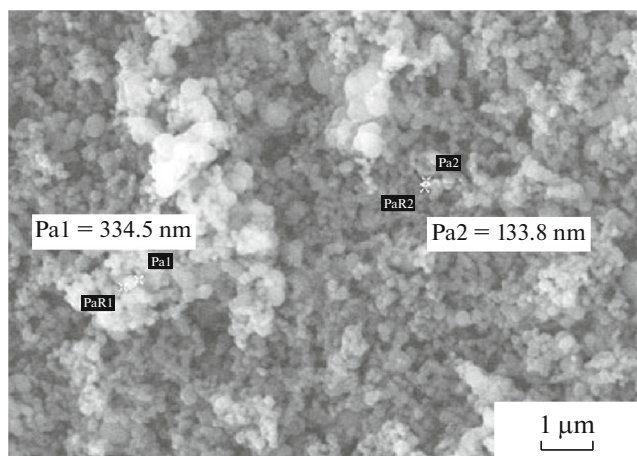


Fig. 4. SEM image of silicon oxonitride particles $\text{Si}_2\text{N}_2\text{O}$.

results of the chemical analysis, the content of elements in the samples of powders is 50 wt % silicon, 24 wt % nitrogen, and 28–32 wt % oxygen. Concentration of the doping oxide (lanthanum oxide) is 0.2 wt %. These data are in complete agreement with the composition of silicon oxonitride $\text{Si}_2\text{N}_2\text{O}$ with an excess in the oxygen content, which is associated with the presence of silicon oxide impurities in the material.

The IR absorption spectrum of $\text{Si}_2\text{N}_2\text{O}$ powders obtained in the experiments confirms the presence of chemical bonds of the main elements. The most intense absorption bands observed are ascribed as follows: at 948 cm^{-1} , to the stretching vibrations of the Si–N bonds (950 cm^{-1}) in the Si_3N group; a wide band with a maximum at 1074 cm^{-1} , to stretching vibrations of the Si–O bond in Si–O–Si fragments. A less intense band with a maximum at 473.9 cm^{-1} is due to vibrations of Si–N bonds. A wide band with a maximum at 3330 cm^{-1} can be attributed to stretching vibrations of N–H bonds (3390 cm^{-1}) [32–34].

Thus, the preparation of doped silicon oxonitride by pyrolysis using gas-droplet input is possible under the following conditions: the size of the drops of raw material does not exceed 0.05 mm; the maximum diameter of the cone of the spray torch should not be more than 0.8 of the inner diameter of the reactor; the gas flow rate should provide the residence time of the reagents in the reactor of at least 0.8–1 s with a ratio of its diameter to the length of 1 : 12–1 : 14; the process temperature is 1000–1100°C; complete conversion is achieved when the ammonia content in the gas phase is 0.5–0.6 mol per 1 mol of the initial HMDS. The introduction of alloying additives (REE oxides) to the composite does not have a significant effect on the pyrolysis process in a fairly wide concentration range.

In addition to the $\text{Si}_2\text{N}_2\text{O}$ powders considered above, single-phase powders of alpha-modification of silicon nitride Si_3N_4 are obtained in the form of

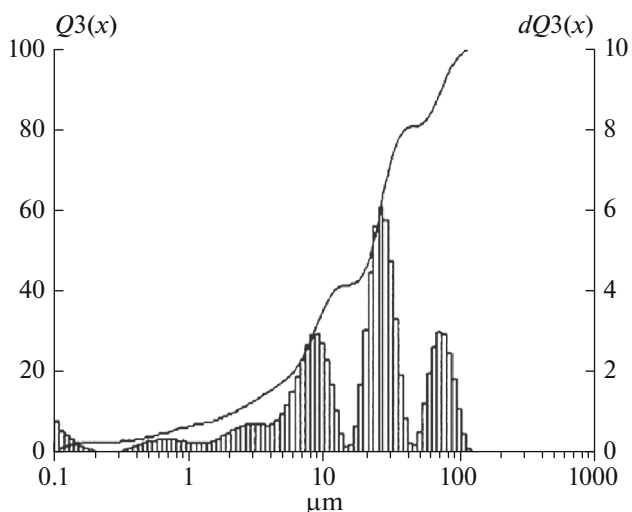


Fig. 5. Particle size distribution of silicon oxonitride powder.

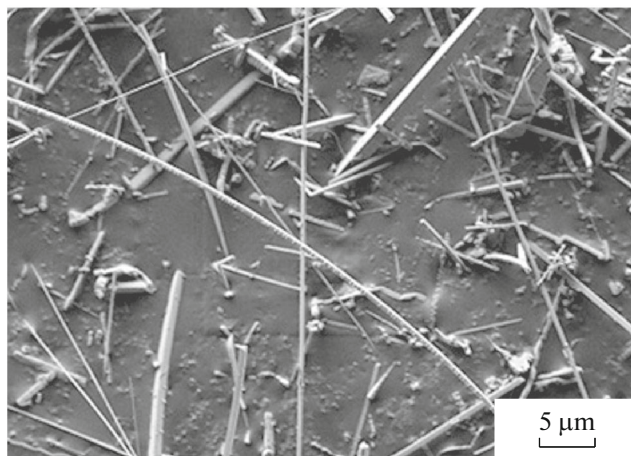


Fig. 6. Si_3N_4 whiskers obtained by gas-phase pyrolysis of hexamethyldisilazane.

fibrous crystals with a particle diameter of 50–200 nm, length from tens to hundreds of microns, and specific surface area of up to $11\text{ m}^2/\text{g}$ (Fig. 6) by gas-phase pyrolysis of hexamethyldisilazane.

CONCLUSIONS

The conditions for the preparation of amorphous powders of silicon nitride Si_3N_4 and silicon oxonitride $\text{Si}_2\text{N}_2\text{O}$ by gas-phase pyrolysis of hexamethyldisilazane are experimentally studied.

The technique is developed and the installation is done for the implementation of pyrolysis of organometallic compounds in nitrogen–ammonia mixture at temperatures up to 1100°C.

The influence of gas-dynamic conditions of synthesis is studied on the properties of nanopowder silicon oxonitride. The optimal conditions for pyrolysis process are found: temperature, ratio of gas mixture

components, mixing conditions, and phase contact times.

X-ray amorphous Si_3N_4 and $\text{Si}_2\text{N}_2\text{O}$ powders are obtained with particle sizes of 50–200 nm and specific surface up to $15 \text{ m}^2/\text{g}$.

FUNDING

This work was performed according to the State Task of Institute of Metallurgy and Materials Science of the Russian Academy of Sciences, no. 075-00746-19-00.

REFERENCES

- Samsonov, G.V., *Nemetallicheskie nitridy* (Nonmetallic Nitrides), Moscow: Metallurgiya, 1969.
- Andrievskii, R.A. and Spivak, I.I., *Nitrid kremniya i materialy na ego osnove* (Silicon Nitride and Materials Based on It), Moscow: Metallurgiya, 1984.
- Garshin, A.P., Gropyanov, V.M., Zaitsev, G.P., and Semenov, S.S., *Keramika dlya mashinostroeniya* (Ceramics for Mechanical Engineering), Moscow: Nauchtekhlitizdat, 2003.
- Vikulin, V.V., Si_3N_4 -based products and their application in the aerospace industry, *Perspekt. Mater.*, 2006, no. 5, pp. 14–19.
- Shatalin, A.S. and Romashin, A.G., New construction materials based on ceramics and ceramic matrix composites. Part 1: Structural ceramic materials, *Perspekt. Mater.*, 2001, no. 4, pp. 5–16.
- Zhuravleva, N.V. and Lukin, E.S., Ceramics based on silicon nitride: a review, *Refractories*, 1993, vol. 34, nos. 1–2, pp. 13–21.
- Andreeva, M.G., Babii, O.A., Gogotsi, Yu.G., Grigor'ev, O.N., Ikonnik, N.K., Trunov, G.V., and Yaroshenko V.P., Hot pressing, structure, and properties of materials based on silicon nitride, in *Materialy na osnove nitridov* (Nitride-Based Materials), Kiev: Inst. Probl. Materialoved., 1988, pp. 173–181.
- Liu, X.-J., Huang, Zh.-Y., Ge, Q.-M., et al. Microstructure and mechanical properties of silicon nitride ceramics prepared by pressureless sintering with $\text{MgO}-\text{Al}_2\text{O}_3-\text{SiO}_2$ as sintering additive, *J. Eur. Ceram. Soc.*, 2005, vol. 25, no. 14, pp. 3353–3359.
- Becher, P.F., Painter, G.S., Shibata, N., and Satet, R.L., Influence of additives on anisotropic grain growth in silicon nitride ceramics, *Mater. Sci. Eng., A*, 2006, vol. 422, pp. 85–91.
- Lange, F.F., The sophistication of ceramic science through silicon nitride studies, *J. Ceram. Soc. Jpn.*, 2006, vol. 114, pp. 873–879.
- Satet, R.L., Hoffmann, M.J., and Cannon, R.M., Experimental evidence of the impact of rare-earth elements on particle growth and mechanical behavior of silicon nitride, *Mater. Sci. Eng., A*, 2006, vol. 422, pp. 66–76.
- Wani, M.F., Khan, Z.A., and Hadfield, M., Effect of sintering additives and reinforcement on microhardness values of Si_3N_4 ceramics and composites, *J. Adv. Res. Mech. Eng.*, 2010, vol. 1, pp. 52–59.
- Kargin, Yu.F., Lysenkov, A.S., Ivicheva, S.N., Zakorzhevskii, V.V., Borovinskaya, I.P., Kutsev, S.V., and Solntsev, K.A., Hot-pressed Si_3N_4 ceramics containing $\text{CaO}-\text{Al}_2\text{O}_3-\text{AlN}$ modifying additives, *Inorg. Mater.*, 2012, vol. 48, no. 11, pp. 1291–1296.
- Kargin, Yu.F., Ivicheva, S.N., Ovsyannikov, N.A., Lysenkov, A.S., Chernyavsky, A.S., Alad'ev, N.A., and Kutsev, S.V., Nanofibers Si_3N_4 , *Inorg. Mater.*, 2009, vol. 45, no. 5, pp. 511–516.
- Tatli, Z. and Thompson, D.P., Low temperature densification of silicon nitride using Li_2O -based surface coatings, *Ceram. Int.*, 2012, vol. 38, pp. 15–21.
- Perevislov, S.N., Liquid-sintered materials based on silicon nitride with oxide additives in the system $\text{MgO}-\text{Y}_2\text{O}_3-\text{Al}_2\text{O}_3$, *Perspekt. Mater.*, 2013, no. 10, pp. 47–53.
- Perevislov, S.N. and Nesmelov, D.D., Properties of SiC and Si_3N_4 based composite ceramic with nanosize component, *Glass Ceram.*, 2016, vol. 73, nos. 7–8, pp. 249–252.
- Wang, C.M., Pan, X., Rühle, M., Riley, F.L., and Mitomo, M., Silicon nitride crystal structure and observations of lattice defects, *J. Mater. Sci.*, 1996, vol. 31, pp. 5281–5298.
- Tsucuma, K., Shimada, M., and Koisumi, M., Thermal conductivity and microhardness of Si_3N_4 with and without additives, *J. Am. Ceram. Soc. Bull.*, 1981, vol. 60, no. 9, pp. 910–912.
- Andrievskii, R.A. and Lyutikov, R.A., High-temperature dissociation of silicon nitride, *Russ. J. Phys. Chem. A*, 1996, vol. 70, no. 3, pp. 526–528.
- Kopylova, V.P. and Nazarchuk, T.N., Chemical stability of silicon nitride and oxynitride powders, *Sov. Powder Metall. Met. Ceram.*, 1975, vol. 14, no. 10, pp. 812–816.
- Grün, R., The crystal structure of $\beta\text{-Si}_3\text{N}_4$: structural and stability considerations between α - and $\beta\text{-Si}_3\text{N}_4$, *Acta Crystallogr., Sect. B: Struct. Sci., Cryst. Eng. Mater.*, 1979, vol. 35, pp. 800–804.
- Toraya, H., Crystal structure refinement of $\alpha\text{-Si}_3\text{N}_4$ using synchrotron radiation powder diffraction data: unbiased refinement strategy, *J. Appl. Crystallogr.*, 2000, vol. 33, pp. 95–102.
- Hiraga, K., Tsuno, K., Shindo, D., Hirabayashi, M., Hayashi, S., and Hirai, T., Structure of α - and $\beta\text{-Si}_3\text{N}_4$ observed by 1 MV electron microscopy, *Philos. Mag.*, 1983, vol. 47, pp. 483–496.
- Wendel, J.A. and Goddard, W.A., III, The Hessian biased force field for silicon nitride ceramics: predictions of thermodynamic and mechanical properties for α - and $\beta\text{-Si}_3\text{N}_4$, *J. Chem. Phys.*, 1992, vol. 97, pp. 5048–5062.
- Yunushev, A.S., Shock-wave synthesis of cubic silicon nitride, *Combust., Explos. Shock Waves* (Engl. Transl.), 2004, vol. 40, no. 3, pp. 370–373.
- Zerr, A., Miehe, G., Serhgiou, G., Schwarz, M., Kroke, E., Riedel, R., Fuess, H., Kroll, P., and Boehler, R., Synthesis of cubic silicon nitride, *Nature*, 1999, vol. 400, pp. 340–342.
- Schwarz, M., Miehe, G., Zerr, A., Kroke, E., Poe, B.T., Fuess, H., and Riedel, R., Spinel- Si_3N_4 : multi-anvil press synthesis and structural refinement, *Adv. Mater.*, 2000, vol. 12, pp. 883–887.

29. Fainer, N., Rumyantsev, Yu., Kosinova, M., Maximovskii, E., Kesler, V., Kirienko, V., and Kuznetsov, F., Low-k dielectrics on base of silicon carbon nitride films, *Surf. Coat. Technol.*, 2007, vol. 201, no. 22, pp. 9269–9274.
30. Herlin, N., Luce, M., Musset, E., and Cauchetier, M., Synthesis and characterization of nanocomposite Si/C/N powders by laser spray pyrolysis of hexamethyldisilazane, *J. Eur. Ceram. Soc.*, 1994, vol. 13, no. 4, pp. 285–291.
31. Ge, K.K., Ye, L., Han, W.J., Han, Y., and Zhao, T., Pyrolysis of polyborosilazane and its conversion into SiBN ceramic, *Adv. Appl. Ceram.*, 2014, vol. 113, no. 6, pp. 367–371.
32. Nakamoto, K., *Infrared and Raman Spectra of Inorganic and Coordination*, Chichester: Wiley, 1970.
33. Peter, S., Bernütz, S., Berg, S., and Richter, F., FTIR analysis of α -SiCN:H films deposited by PECVD, *Vacuum*, 2013, vol. 98, pp. 81–87.
34. Tomar, V.K., Patil, L.S., and Gautam, D.K., Deposition and characterization of silicon nitride films using HMDS for photonics applications, *J. Optoelectron. Adv. Mater.*, 2008, vol. 10, no. 10, pp. 2657–2662.

Translated by Sh. Galyaltdinov